

古気候復元における成層圏オゾンの影響: MRI-ESM による完新世中期実験 Impact of stratospheric ozone on paleoclimate reconstruction: Mid-Holocene experiment by using MRI Earth System Model

納多 哲史¹; 水田 亮²; 出牛 真²; 小寺 邦彦³; 吉田 康平²; 鬼頭 昭雄⁴; 村上 茂教⁵; 足立 恭将²;
余田 成男^{1*}

NODA, Satoshi¹; MIZUTA, Ryo²; DEUSHI, Makoto²; KODERA, Kunihiko³; YOSHIDA, Kohei²; KITO, Akio⁴;
MURAKAMI, Shigenori⁵; ADACHI, Yukimasa²; YODEN, Shigeo^{1*}

¹ 京都大学大学院 理学研究科, ² 気象研究所, ³ 名古屋大学 太陽地球環境研究所, ⁴ 筑波大学 生命環境系, ⁵ 気象大学校
¹Graduate School of Science, Kyoto University, ²Meteorological Research Institute, ³Solar-Terrestrial Environment Laboratory,
Nagoya University, ⁴Graduate School of Life and Environmental Sciences, University of Tsukuba, ⁵Meteorological College

Numerical experiment of mid-Holocene (6000 years before present) is performed by using Meteorological Research Institute Earth System Model (MRI-ESM) to investigate the impact of ozone distribution which is modulated by orbital elements on the tropospheric climate. The result of interactive ozone calculation is compared to those of mid-Holocene and pre-industrial control experiments in CMIP5/PMIP3, in which the ozone distribution was fixed to the value of 1850. Contribution of the chemical processes shows anomaly up to +1.7 K in the Antarctic regions for the annual mean zonal mean temperature at 2 m from the surface. This impact is caused by decrease in the area of sea ice, and the interrelationship in the trend is found to be opposite to that of sea ice and the Antarctic ozone hole as observed in these decades.

Stratospheric warming in the Antarctic spring due to the positive anomaly of ozone causes negative westerly anomaly of the polar night jet by the thermal wind balance, and the annular mode response brings westerly anomaly near the surface. The decrease of the surface westerly weakens the northward component of the Ekman transport in the ocean, suppresses the sea ice transport to lower latitudes, and produces the warming in the polar region.

The importance of chemical feedbacks is supported by a correction of cold bias of SST in the southern hemisphere which is commonly seen in results of CMIP5/PMIP3 models. The comparison between the time variation of the sea ice distribution and that of the stratosphere-troposphere coupling patterns show the importance of coupled chemistry process related to ozone in the reconstruction of mid-Holocene climate.

キーワード: オゾン, 太陽放射, 古気候, 地球システムモデル, 海氷

Keywords: ozone, solar radiation, paleoclimate, earth system model, sea ice

極域熱圏・電離圏の基本構造 Climatology of the polar thermosphere and ionosphere

藤原均^{1*}; 三好勉信²; 陣英克³; 品川裕之³; 野澤悟徳⁴; 小川泰信⁵; 片岡龍峰⁵
FUJIWARA, Hitoshi^{1*}; MIYOSHI, Yasunobu²; JIN, Hidekatsu³; SHINAGAWA, Hiroyuki³;
NOZAWA, Satonori⁴; OGAWA, Yasunobu⁵; KATAOKA, Ryuhô⁵

¹ 成蹊大学 理工学部, ² 九州大学 大学院理学研究院, ³ 情報通信研究機構, ⁴ 名古屋大学 太陽地球環境研究所, ⁵ 国立極地研究所

¹Faculty of Science and Technology, Seikei University, ²Department of Earth and Planetary Sciences, Faculty of Sciences, Kyushu University, ³National Institute of Information and Communications Technology, ⁴Solar Terrestrial Environment Laboratory, Nagoya University, ⁵National Institute of Polar Research

Recent observations from satellites and ground-based instruments have clarified various phenomena in the polar thermosphere and ionosphere, in particular, the cusp and polar cap region. The CHAMP satellite observations for a decade were the great success to understand the mass density variations in the global thermosphere. However, some basic features and/or climatology of the polar thermosphere and ionosphere seem to be still unknown. For example, amplitudes of the temperature and wind variations during a solar cycle are not exactly known in the local area in and/or in the vicinity of the cusp/polar cap region. In addition, contributions of the lower atmosphere to the temperature and wind variations in the thermosphere seem not to be understood quantitatively in each local area. In order to understand climatology of the polar thermosphere and ionosphere, we have made some observations with the EISCAT radar system and optical instruments in 2011-2015 and performed numerical simulations with a whole atmosphere GCM. The five-year observations of the polar ionosphere with the EISCAT radar system show the large difference between the ionospheres over Longyearbyen and Tromsø; variations of the dayside ion temperature and ion motion at Longyearbyen are larger than those at Tromsø on average during geomagnetically quiet periods. The EISCAT data during the extremely low solar activity 2007-2008 have also clarified the basic state of the ionosphere which would be strongly affected by the lower atmosphere. We will show the recent progress of our understandings of basic features of the polar thermosphere and ionosphere from the observations and GCM simulations.

キーワード: 熱圏, 電離圏, 極域, EISCAT, GCM, シミュレーション

Keywords: thermosphere, ionosphere, polar region, EISCAT, GCM, simulation

GAIAを用いたスプラディックE層出現特性の解析 Analysis of occurrence characteristics of sporadic E layers using GAIA

品川 裕之^{1*}; 三好 勉信²; 陣 英克¹; 藤原 均³

SHINAGAWA, Hiroyuki^{1*}; MIYOSHI, Yasunobu²; JIN, Hidekatsu¹; FUJIWARA, Hitoshi³

¹ 情報通信研究機構, ² 九州大学, ³ 成蹊大学

¹NICT, ²Kyushu University, ³Seikei University

スプラディックE層(Es)は、高度約90kmから120kmの間の領域に存在する非常に薄く高密度のイオン層である。Esは、短波を利用した通信や放送に大きな影響を及ぼすことが知られており、宇宙天気予報においては重要な現象の一つである。Esは、基本的には下部熱圏、上部中間圏付近の中性風のシアと流星起源の金属イオンの組み合わせによってできると考えられているが、その形成や変動過程は定量的にはまだ十分に解明されていない。これまでの観測から、Esは季節変動、地方時変動、地理的な場所の依存性などを示すことが分かっている。中でも特徴的なのは、Esが北半球の夏には東アジアの中緯度付近で最も多く発生し、南半球の夏には南アメリカの中緯度付近で最も多く発生することである。この現象は観測的には古くから知られていたが、今日まで理論的に解明されていなかった。我々のグループでは、全大気圏と電離圏を矛盾なく結合し、下層大気に気象庁の再解析データを入力したモデル(GAIA: Ground-to-topside model of Atmosphere and Ionosphere for Aeronomy)の開発を行ってきた。このモデルは、Esの構造を直接再現するにはまだ分解能が十分とは言えないが、Esの発生条件を大まかに見積もることは可能である。今回は、GAIAのシミュレーションデータを用いてE領域の中性風シアの解析を行った。その結果、風のシアは、これまでの観測で得られたEsの出現特性とほぼ同じく、北半球の夏には東アジアの中緯度付近で最も大きく、南半球の夏では南アメリカの中緯度付近で最も強くなることが分かった。本発表では、この中性風シア発生頻度の地域依存性のメカニズムについて議論する。

キーワード: スプラディックE層, 大気圏, 電離圏, モデル, 中性風シア, 発生

Keywords: sporadic E layer, atmosphere, ionosphere, model, neutral wind shear, occurrence

Introduction of long-term whole atmosphere-ionosphere simulation database and future update

Introduction of long-term whole atmosphere-ionosphere simulation database and future update

陣 英克^{1*}; 三好 勉信²; 藤原 均³; 品川 裕之¹; Matsuo Tomoko⁴
JIN, Hidekatsu^{1*}; MIYOSHI, Yasunobu²; FUJIWARA, Hitoshi³; SHINAGAWA, Hiroyuki¹; MATSUO, Tomoko⁴

¹ 情報通信研究機構, ² 九州大学, ³ 成蹊大学, ⁴ 米国大気海洋庁

¹National Institute of Information and Communications Technology, ²Kyushu University, ³Seikei University, ⁴National Oceanic and Atmospheric Administration

超高層大気領域は人工衛星や地上 - 衛星間をつなぐ電波の通り道であり、その擾乱や変動は衛星の軌道や姿勢、また電波の伝搬に影響する。超高層大気の擾乱や変動の起源は、太陽フレアなど太陽面の活動が磁気圏を通して入ってくるだけではなく、地表付近の気象の影響も中層大気を通り入ってくることで知られてきた。我々は、電離圏・熱圏の全球分布を将来的に数値的に推測・予測するために、地表から熱圏上部までの中性大気領域と電離圏領域を相互に結合する大気圏電離圏結合モデル (GAIA) を開発してきた。さらに、現実の太陽放射強度の変動として日々の F10.7 を入力する以外に、モデルの下層大気領域に気象再解析データをナッジング手法により取り込み、現実の気象活動の影響による超高層大気変動を再現する試みを行ってきた。本発表では、1996 年から 2014 年まで行った気象再解析データを取り入れた大気圏電離圏シミュレーションのデータベースについて紹介する。データベースでは、太陽活動と自転に伴う変動のほかに、電離圏と熱圏の季節変動や、より周期の短い下層大気起源の周期的変動が見られている。また、下層大気の突発的な擾乱に伴う超高層大気の擾乱も再現されている (Jin et al, 2012; Liu et al., 2013, 2014)。本発表では、シミュレーションデータベースと観測との比較について報告する。また、今後モデルの精度向上に向けてデータ同化手法を取り入れようとしており、その試みについて紹介する。

キーワード: 宇宙天気, 電離圏, データ同化, データベース, 熱圏, シミュレーション

Keywords: space weather, ionosphere, data assimilation, database, thermosphere, simulation

Beacon experiment of the ionosphere in Japan and southeast Asia Beacon experiment of the ionosphere in Japan and southeast Asia

山本 衛^{1*}
YAMAMOTO, Mamoru^{1*}

¹ 京都大学生存圏研究所
¹ RISH, Kyoto University

We have been successfully conducted observations of total-electron content (TEC) of the ionosphere by the satellite-ground beacon experiment. An unique dual-band (150/400MHz) digital receiver GRBR (GNU Radio Beacon Receiver) were developed based on the recent digital signal processing technologies. The GRBR receivers were deployed first in Japan, and then in southeast Asia, and other areas. Data from the GRBR network were used for the investigations of variety of ionospheric phenomena. We have found mid-latitude summer nighttime anomaly (MSNA) over Japan, which is summer nighttime TEC enhancement at higher latitudes. Longitudinal "large-scale wave structures (LSWS)" in the low latitude were studied in detail as a source of equatorial Spread-F (ESF) events. Also we were successful to measure the equatorial ionospheric anomaly (EIA) near 100E longitude in large latitudinal extent of at most +/-20 degrees around the geomagnetic equator. The technique is utilized for sounding rocket-ground experiment as well. We review the ionospheric studies with the GRBR network, and will discuss future direction of the related studies.

キーワード: 衛星-地上ビーコン観測, 全電子数, 中低緯度電離圏, GRBR 観測網

Keywords: Satellite-ground beacon experiment, Total electron content, Middle- and low-latitude ionosphere, GRBR network

Statistical analyses on the thermal plasma density of the plasmasphere from the Akebono PWS observation

Statistical analyses on the thermal plasma density of the plasmasphere from the Akebono PWS observation

長谷川 周平¹; 三好 由純^{1*}; 北村 成寿¹; 桂華 邦裕¹; 小路 真史¹; 熊本 篤志²; 町田 忍¹
HASEGAWA, Shuhei¹; MIYOSHI, Yoshizumi^{1*}; KITAMURA, Naritoshi¹; KEIKA, Kunihiro¹; SHOJI, Masafumi¹; KUMAMOTO, Atsushi²; MACHIDA, Shinobu¹

¹ 名古屋大学太陽地球環境研究所, ² 東北大学大学院理学研究科地球物理学専攻

¹Solar-Terrestrial Environment Laboratory, Nagoya University, ²Department of Geophysics, Graduate School of Science, Tohoku University

The plasmasphere is a region of cold and dense plasma surrounding the Earth. The thermal plasma density of the plasmasphere is an important parameter for understanding the dynamics of the radiation belts as well as the inner magnetosphere, because the thermal plasma density controls the wave-dispersion relation, resonance conditions, etc. In this study, we conduct statistical analyses on the variations of the plasmasphere and plasmatrough, using electron density data derived from long-term plasma wave observations by the PWS experiments on board the Akebono satellite. We investigate the solar cycle variations of the thermal plasma density distribution. In deep plasmasphere, the thermal plasma density distributions along the field line do not significantly change during the solar cycle, and their distributions are well modeled as the diffusive equilibrium. On the other hand, the thermal plasma density distributions drastically change during the solar cycle in the outer portion of the plasmasphere. The thermal plasma density distributions are similar to the collisionless model during the solar active periods, while those are similar to the diffusive equilibrium model during the solar quiet periods. We also investigate time variations of the plasmaspheric density distribution during geomagnetic storms driven by CMEs and CIRs with superposed epoch analyses. The zero time corresponds to the minimum of the Dst index. The plasmaspheric density shrinkage depends on the storm amplitudes. The recovery time of the thermal plasma density is significantly different between CME- and CIR-storms. During the recovery phase of CIR-storms, the plamapause does not recover quickly because of prolonged substorm activities during the high-speed streams. The recovery rates of the thermal plasma density depend on the L-shell, which is consistent with the previous studies. We find that the recovery rates of CME-storms are larger than that of CIR-storms.

Keywords: plasmasphere, electron density, akebono satellite, solar-cycle, geomagnetic storm

太陽活動領域：誕生から噴出まで Solar Active Regions: From Birth to Eruption

鳥海 森^{1*}
TORIUMI, Shin^{1*}

¹ 国立天文台
¹National Astronomical Observatory of Japan

Solar-terrestrial environment is largely influenced by flares and CMEs sourced from the Sun. In particular, stronger events are known to be produced from solar active regions (ARs) including sunspots. Therefore, it is of great importance to understand the creation mechanism of ARs and their relationship with solar eruptions. Now it is widely accepted that ARs are caused by emerging magnetic flux, which is created by the dynamo effect in the convection zone. As a result of this flux emergence, several magnetic elements of the same polarity merge together at the solar surface and eventually form a single sunspot. Observations have revealed that large and complex ARs, the so-called delta sunspots, produce stronger flares. This may be because the free magnetic energy (or non-potentiality) is stored in such complex, sheared ARs with larger magnetic flux. Recent developments in the numerical modeling of flux emergence and flare eruptions open the door to further understanding of physical mechanisms behind such events. For example, our numerical simulations suggest that the flare-productive quadrupolar AR NOAA 11158, which is responsible for many X- and M-class flares, is produced from a single flux tube that is greatly disturbed in the convection zone during its emergence process. In this presentation, motivated by the above scientific curiosity, we review the observational and theoretical progress in the field of flux emergence, AR formation including delta-sunspots, and the resultant triggering of flare eruptions. After that, we discuss the future prospects.

Keywords: the Sun, active region, flux emergence, flare, MHD

太陽フレアのトリガ過程に関する観測的研究 Observational Study of the Flare Trigger Process

伴場 由美^{1*}; 草野 完也¹
BAMBA, Yumi^{1*}; KUSANO, Kanya¹

¹ 名古屋大学太陽地球環境研究所
¹ STEL/Nagoya Univ.

Solar Flares are explosive phenomena driven by magnetic energy stored in the solar corona. Because interplanetary disturbances associated with solar flares sometimes impact terrestrial environments and infrastructure, understanding the flare-triggering mechanism is important not only from a solar physics perspective but also for space weather forecasting. There are numerous observational studies and numerical simulations which attempted to reveal the onset mechanism of solar flares. However, because different observations support different models, the underlying mechanism of flare onset remains elusive, and the predictability of flare occurrence is limited.

To elucidate flare-trigger mechanism, Bamba et al. 2013 investigated four major flare events that occurred in active regions NOAA 10930 and NOAA 11158. We used data obtained by the Solar Optical Telescope (SOT) onboard the Hinode satellite. We analyzed the spatio-temporal correlation between the detailed magnetic field structure and the emission image of the Ca II H line at the central part of flaring regions for several hours prior to the onset of flares. We observed that characteristic magnetic disturbances developed at the centers of flaring regions in the pre-flare phase. These magnetic disturbances can be classified into two groups depending on the structure of their magnetic polarity inversion lines; to the so-called "Opposite-Polarity (OP)" and "Reversed-Shear (RS)" magnetic field recently proposed by Kusano et al. 2012. The result strongly suggests that some major flares are triggered by rather small magnetic disturbances. We also show that the critical size of the flare-trigger field varies among flare events and briefly discuss how the flare-trigger process depends on the evolution of active regions.

Because of the limitation of SOT field of view, however, only four events in the Hinode data sets have been utilizable in our previous study. Therefore, increasing the number of events is required for evaluating the flare trigger model. Bamba et al. 2014 investigated the applicability of data obtained by the Solar Dynamics Observatory (SDO) to increase the data sample for a statistical analysis of the flare trigger process. SDO regularly observes the full disk of the sun and all flares although its spatial resolution is lower than that of Hinode. We investigated the M6.6 flare which occurred on 13 February 2011 and compared the analyzed data of SDO with the results of Bamba et al. 2013 using Hinode/SOT data. Filter and vector magnetograms obtained by the Helioseismic and Magnetic Imager (HMI) and filtergrams from the Atmospheric Imaging Assembly (AIA) 1600Å were employed. From the comparison of small-scale magnetic configurations and chromospheric emission prior to the flare onset, we confirmed that the trigger region is detectable with the SDO data. We also measured the magnetic shear angles of the active region and the azimuth and strength of the flare-trigger field. The results were consistent with Bamba et al. 2014. We concluded that statistical studies of the flare trigger process are feasible with SDO as well as Hinode data.

2012年3月7日 X5.4/X1.3 フレア: エネルギーの蓄積・トリガー・解放を探る X5.4/X1.3 flares on 7 March 2012: Exploring the energy storage, trigger and release of solar flares

清水 敏文^{1*}; 井上 諭²

SHIMIZU, Toshifumi^{1*}; INOUE, Satoshi²

¹ 宇宙航空研究開発機構宇宙科学研究所, ² 名古屋大学太陽地球環境研究所

¹ ISAS/JAXA, ² STE laboratory, Nagoya University

太陽フレアは、磁力線の捻れとしてコロナに蓄積された自由エネルギーが突発的に解放され、場合によっては宇宙空間へコロナプラズマの噴出を伴う。本講演では、2012年3月に太陽面に存在した活動領域 11429 に注目する。2012年3月7日には X5.4 および X1.3 フレアを起こし、これらのフレアは VarSITI/ISEST のスタディケースの一候補でもある。このフレアに伴うコロナ質量放出 (CME) は惑星間空間に伝播して、地球では3月9日に大きな磁気嵐を発生させている。この活動領域は δ 型黒点を含み、領域全体が強くシアしている。理解に乏しいフレアのトリガー機構を学術的に理解することは、宇宙天気フレア発生予測にとって重要である。シアした磁場構造に対して、その磁気中性線上に小さなトリガ磁場が「反シア型」に成長することが、フレア発現の一つの磁場形態であると指摘されている。「ひので」可視光磁場望遠鏡 (SOT) の高精度磁場観測によって、X5.4 フレアに対する「反シア型」のトリガ磁場が磁気中性線上に特定されている。さらに、「ひので」の磁場および速度場観測から、1) トリガ磁場の横に、小さな双極の磁場が磁気中性線に沿って形成され、フレア発生の少なくとも6時間以上前から激しい音速ガス流がその磁場に沿って励起されていること、2) 激しいガス流が徐々に双極の磁場を成長させ、その先に存在したトリガ磁場を徐々に押して、トリガ条件の磁場構造に向けて磁場配置を変化させていること、等を発見した。この観測結果は、光球ガスのダイナミクスがフレア発現のトリガに至らしめる上で重要な役割を果たしていることを示唆している。一方、その約1時間後に、同じ磁気中性線に沿った西側の領域で、X1.3 フレアが発生し、アーケード状の X 線構造が発達する。なぜ、一度に系全体の磁場が噴出せずに、2段階になったのだろうか？ X5.4 フレアに対して激しい光球ガスのダイナミクスが特定されたが、X1.3 フレアの発現には光球ガスのダイナミクスがどのように関わっているのだろうか？ 光球ベクトル磁場に基づいた NLFFF モデリングによってコロナ磁場の形状を推定し、ねじれ磁場の空間分布を導出した。各フレアの足下に現れるフレアリボン構造から、エネルギー解放が起きた磁力線を時間的にトレースして、ねじれコロナ磁場のどの部分が噴出したのかを評価した。この活動領域の磁場特徴やダイナミクスを示して、フレア蓄積と発現について議論する。

キーワード: 太陽フレア, ひので, 光球磁場, コロナ, コロナ磁場, 宇宙天気

Keywords: Solar flare, Hinode, Photospheric magnetic field, corona, coronal field, space weather

4重極磁場構造におけるホモロガスフレア Homologous flare occurred at the quadrupole field

川畑 佑典^{1*}; 清水 敏文²

KAWABATA, Yusuke^{1*}; SHIMIZU, Toshifumi²

¹ 東京大学大学院理学系研究科地球惑星科学専攻, ² 宇宙航空研究開発機構宇宙科学研究所

¹Department of Earth and Planetary Science, The University of Tokyo, ²Institute of Space and Astronautical Science, JAXA

Many models of the solar flare are suggested and they can explain some of the observed flares. However, they cannot explain all of the observed flares. The purpose of our study is investigating such events. We focus on homologous flares, which occur at the same location in the same active region repeatedly. We used Solar Optical Telescope (SOT) on board *Hinode* and Atmospheric Imaging Assembly (AIA) on board *Solar Dynamics Observatory (SDO)*. We can obtain three dimensional vector of the magnetic field by using the spectropolarimetric data of SOT and investigate the coronal configurations by using the extreme ultraviolet data of AIA. We analyze the active region NOAA 11967 which produced three M class flares on 2014 February 2. These flares show homology and the magnetic field at the flaring region is quadrupole. There were four flare ribbons and they showed rapid slipping motion. The photospheric flow can be seen between the sunspot and this flow may play a role in storing free energy and triggering the flare.

キーワード: 太陽フレア, 磁気リコネクション

Keywords: solar flare, magnetic reconnection

Study on the Solar Flare Trigger Mechanism by using 3D Data Driven Magnetohydrodynamic Simulations

Study on the Solar Flare Trigger Mechanism by using 3D Data Driven Magnetohydrodynamic Simulations

MUHAMAD, Johan^{1*} ; KUSANO, Kanya¹ ; INOUE, Satoshi¹
MUHAMAD, Johan^{1*} ; KUSANO, Kanya¹ ; INOUE, Satoshi¹

¹STEL, Nagoya University

¹STEL, Nagoya University

Solar Flare can unleash large amount of energy from the Sun into the solar system and may affect global space based technologies on Earth. However, the detail process of the solar flare mechanism, especially in the early phase of the flare, is still not completely understood. It is believed that initially flare takes place from the highly sheared magnetic field in the active region of the Sun which contains very large non-potential energy. This strong sheared field is then destabilized by some trigger processes which responsible in releasing the free energy through some eruptions.

Several results from the previous numerical simulation study (Kusano et al., 2012) suggested that small magnetic flux which is imposed to the various simple magnetic structures can trigger the eruptions. Two different types of small magnetic structures near the polarity inversion line (PIL) are suggested as the possible configurations for the trigger of flares. They are the small bi-pole fields of opposite polarity or reversed shear compared to the highly sheared magnetic field in the scale of active region. Started from this result, we extend this work by using more realistic configuration of magnetic fields which mimic the solar coronal magnetic structure.

In this presentation, we will present some results of our simulations to elucidate the trigger process of solar eruption based on the 3D magnetohydrodynamic (MHD) model. In order to do this, we perform Nonlinear Force Free Field (NLFFF) extrapolation (Inoue et al., 2014) using the vector magnetogram data of the active region NOAA 10930 from the Hinode satellite. The NLFFF of the active region before the eruption showed that strong sheared magnetic field appeared near the PIL. We systematically carried out the numerical simulations, in which several emerging fluxes are injected onto different points in the NLFFF. As a result, we confirmed that some types of small emerging flux can trigger the eruption. It verifies that the previous work mechanism (Kusano et al. 2012) can be applied to more realistic magnetic structure. Our result suggests that the position and intensity of the emerging flux with respect to the initial NLFFF condition is very crucial for triggering the solar eruption.

References:

[1] Magnetic Field Structures Triggering Solar Flares and Coronal Mass Ejections,
K. Kusano, Y. Bamba, T. T. Yamamoto, Y. Iida, S. Toriumi, and A. Asai,
2012 ApJ 760 31 doi:10.1088/0004-637X/760/1/31

[2] Nonlinear Force-Free Extrapolation of the Coronal Magnetic Field Based on the Magnetohydrodynamic Relaxation Method,
Inoue, S., Magara, T., Pandey, V. S., Shiota, D., Kusano, K., Choe, G. S., Kim, K. S.,
2014 ApJ 780 101 doi:10.1088/0004-637X/780/1/101

キーワード: Solar Flare, MHD Simulation, Nonlinear Force Free Field, Active Region
Keywords: Solar Flare, MHD Simulation, Nonlinear Force Free Field, Active Region

大振幅地磁気急始変化 (SC) の性質 Properties of large amplitude geomagnetic sudden commencement (SC)

荒木 徹^{1*}; 新堀 淳樹²
ARAKI, Tohru^{1*}; SHINBORI, Atsuki²

¹ 中国極地研究所, ² 京都大学生存圏研究所

¹Polar Research Institute of China, ²Research Institute for Sustainable Humanosphere, Kyoto University

Araki[2014, EPS] は, 1868 年以降の SC 振幅を調べ, 1940 年 3 月 24 日の SC が最大であることを確かめた. この SC の振幅 ΔH は, 柿岡で 273nT 以上, Alibag で 310nT であった. Siscoe et al. [1968] の, SC 振幅 ΔH と太陽風動圧 Pd の関係式, $\Delta H = \alpha \Delta (\sqrt{Pd})$ [$\alpha = f g k$, k; 比例係数, f; 太陽風と磁気圏の相互作用に関わる係数 (~1-2), g; 地下誘導電流効果 (~1.5)] を使うと, 対応する Pd 増加は 400-500nPa になる. これは 1868 年以降最大の惑星間空間衝撃波 (IPS) に伴う Pd であるから, 出来るだけ精密に決めたい (線形近似の妥当性の議論は別に必要である).

磁気圏圧縮の際には, 磁気圏界面電流 (MPC) の増加と共に沿磁力線電流 (FAC)・電離層電流 (IC) が誘起されて SC 振幅に LT 変化を生じさせ, それに応じて上記の比例係数 k も LT 変化を示す [新堀, 2014]. SC 振幅 ΔH から対応する Pd 変化を求める際には, この LT 変化を考慮する必要がある.

通常 2nPa 程度の Pd が 30nPa を越すと磁気圏界面は静止軌道の内側に入って来る. その時の MPC, FAC, IC の地上磁場への寄与の割合が, Pd が小さい時に比べて異なり, SC 振幅 LT 変化も異なることが予想される. したがって, 大振幅 SC の LT 変化を調べ, それを IPS-Pd の推定に反映させることに意味が出てくる. ここでは, 振幅の LT 変化を中心に, 大振幅 SC の性質を調べる.

柿岡や Alibag では, 50nT 以上の SC の発生率は 5 % 以下, 100nT 以上は 1 % 以下になるので, 統計的解析は出来ない. 多点同時観測のデータ解析を行う.

キーワード: 地磁気急始変化 (SC), 惑星間空間衝撃波, LT 変化, 大振幅

Keywords: geomagnetic sudden commencement(SC), interplanetary shock, LT variation, large amplitude

Progress in Understanding the Earth-affecting Coronal Mass Ejections Progress in Understanding the Earth-affecting Coronal Mass Ejections

Gopalswamy Nat^{1*}
GOPALSWAMY, Nat^{1*}

¹NASA Goddard Space Flight Center
¹NASA Goddard Space Flight Center

Coronal mass ejections (CMEs) producing solar energetic particle (SEP) events at Earth and causing geomagnetic storms are obviously the Earth-affecting CMEs. The occurrence of SEP events depends on the outer structure of CMEs, viz. the MHD shock, irrespective of the internal structure. On the other hand, geomagnetic storms occur when the internal magnetic structure of CMEs and/or the sheath behind the shock contain southward-pointing magnetic fields. The source locations of these two types of CMEs are also different: SEP events require magnetic connectivity to Earth, whereas storm-producing CMEs need to be directed toward Earth. Observations from the STEREO mission have contributed enormously to the study of Earth-affecting CMEs because of the expanded field of view and viewing angles away from the Sun-Earth line. The increased field of view closer to the Sun helped us understand that shocks can form as close as about 1.25 solar radii from the Sun center. The onset of type II radio bursts associated with CMEs has shown that shocks can form at large distances from the Sun (tens of solar radii). SEPs are energized as soon as the shock forms and can continue until the shock arrival at Earth and even afterwards. Therefore, predicting SEP events is generally very difficult (there is little lead time). There is definitely 1-4 days of lead time in predicting geomagnetic storms. There have been many attempts to predict the shock arrival using CME, Type II radio, and IPS observations. The CME trajectory can be severely affected by nearby coronal holes, non-radial ejection, and preceding CMEs resulting in large deviations in the predicted arrival times. We are far from predicting the orientation and strength of the CME magnetic field, which is crucial in predicting the occurrence and strength of geomagnetic storms. Then there are problems like the extremely mild space weather during solar cycle 24. Even though there are sufficiently large number of energetic CMEs ejected from the Sun, they do not seem to produce very many high-energy SEP events and large geomagnetic storms. It appears that this strange behavior can be attributed to a combination of weak solar activity and CME propagation in the altered heliosphere. This talk summarizes some of these issues related to Earth-affecting CMEs and how the issues will be tackled by the ISEST/MiniMax24 project of the SCOSTEP/VarSITI program.

キーワード: Coronal mass ejections, Solar Energetic Particle Events, Geomagnetic Storms, CME propagation, Solar Cycle, SCOSTEP/VarSITI
Keywords: Coronal mass ejections, Solar Energetic Particle Events, Geomagnetic Storms, CME propagation, Solar Cycle, SCOSTEP/VarSITI

GEMSIS-Sun: Numerical Modeling of Sun-Earth System on the Basis of Solar Observations (SUSANOO)

GEMSIS-Sun: Numerical Modeling of Sun-Earth System on the Basis of Solar Observations (SUSANOO)

塩田 大幸^{1*}; 片岡 龍峰²; 三好 由純¹; 草野 完也¹; 山野内 雄哉¹
SHIOTA, Daikou^{1*}; KATAOKA, Ryuho²; MIYOSHI, Yoshizumi¹; KUSANO, Kanya¹; YAMANOUCHI, Yuya¹

¹名古屋大学 太陽地球環境研究所, ²国立極地研究所

¹Solar-Terrestrial Environment Laboratory, Nagoya University, ²National Institute of Polar Research

Solar wind including coronal mass ejections (CMEs) is a main driver of various space weather disturbances. MHD modeling of the solar wind is a powerful tool to understand the solar-terrestrial environment and to forecast space weather accurately. Recently, we have developed an MHD model of the inner heliosphere on the basis of minimal input, namely, time series of daily synoptic observation of the photospheric magnetic field [Shiota et al. 2014]. The time series of MHD parameters at the Earth position is passed to a radiation belt model [Miyoshi et al. 2004] for forecasting of the radiation belt energetic electron flux. These programs are executed everyday on a server in STEL, Nagoya University and the results are uploaded on the web site (<http://st4a.stelab.nagoya-u.ac.jp/susanoo/>). This system is named as Space-weather-forecast-Usable System Anchored by Numerical Operations and Observations (SUSANOO). The calculated time profiles of solar wind velocity and magnetic field at positions of planets agreed with in situ measurements around solar minimum (2007 -2009) [Shiota et al. 2014].

The MHD simulation of solar wind does not include CMEs and therefore this is a possible source of error of the forecast in active period in solar cycle. We have been developing a CME model including magnetic flux ropes [Kataoka et al. 2009]. In the model, each CME is injected as a twisted magnetic flux rope accompanying with a velocity pulse through the inner boundary of the simulation and propagate into the solar winds. Thanks to the including flux ropes, the model is capable for a model of Dst index variation. We attempted to model the solar wind profile when multiple CMEs came from associated recent large-scale active regions: NOAA 10486 in October to November 2003 (Halloween event). As a result, the strength of compressed magnetic field becomes as high as about four times of background IMF when a fast CME interacts with the background solar wind. However, successive CMEs interact with each other to form much stronger magnetic field due to compression of the magnetic cloud of the preceding CME by shock associated the following CME.

キーワード: 太陽風, MHD, 放射線帯, 宇宙天気, コロナ質量放出

Keywords: solar wind, MHD, radiation belt, space weather, CME

太陽風予測モデル SUSANOO-SW の衛星観測との比較による定量的評価 Quantitative Evaluation of Solar Wind Prediction Model "SUSANOO-SW" by Comparison with in-situ Measurements

山野内 雄哉^{1*}; 塩田 大幸¹; 草野 完也¹
YAMANOUCHI, Yuya^{1*}; SHIOTA, Daikou¹; KUSANO, Kanya¹

¹ 名古屋大学 太陽地球環境研究所

¹ Solar-Terrestrial Environment Laboratory, Nagoya University

太陽風の擾乱は、宇宙天気において最も重要な要素の一つである。宇宙天気予報は、地球に到達する前にその擾乱を予測する試みである。現在、最も信頼できる予報では、地球前方に位置する ACE などの探査機の太陽風 in situ 観測が予報に利用されている。しかし、この方法のみでは ACE に到達する前の太陽風の情報は知り得ないため、ACE-地球間を太陽風が伝搬する 1 時間程度のリーディングタイムしか取ることができない。そこで、MHD シミュレーションを用いることで、さらに未来の予測を行うことができる。

近年我々のグループでは、太陽表面磁場のリアルタイム観測データのみを入力として放射線帯の高エネルギー電子の変動を予測する宇宙天気予測モデル SUSANOO (Space-weather-forecast-Usable System Anchored by Numerical Operations and Observations) を開発した。SUSANOO の太陽風モデル (SUSANOO-SW) [Shiota et al. (2014)] は、太陽表面磁場観測データに磁場モデル・経験モデルを適用し、内部太陽圏の太陽風の三次元構造を再現する MHD シミュレーションである。SUSANOO-SW で再現した太陽極小期 (2007~2009 年) の太陽風の惑星の位置での時間変動は、磁場の相関係数が 0.54~0.73、速度の相関係数が 0.40~0.58 と太陽風の in situ 観測をよく再現した [Shiota et al. (2014)]。これは、1 年単位の比較で評価を行ったため、グローバルな太陽風構造の再現性の良さが数字として現れたと理解できる。しかし、より短い時間スケールの詳細な比較を行うと、一部の再現結果が外れていることが確認される。不一致が起きる原因は、SUSANOO-SW の内側境界条件を設定するモデルにあると考えられる。実際の予報に使うためには、さらに精度を高める必要がある。そこで本研究では、SUSANOO-SW モデルと in situ 観測とを詳細に比較し、再現性が悪くなる原因を究明した。

本研究ではまず、SUSANOO-SW モデルを用いて、太陽活動極小期から極大期まで (2007~2014 年) の太陽風変動を計算した。以下の 4 つの基準で観測値との比較をし、モデルの精度を数値化した。(1) Carrington Rotation (CR) ごとの速度変動の相関係数。(2) 速度・磁場変動の一致率:(2-a) 磁場の極性、(2-b) 速度差がしきい値よりも小さいか、(2-c) dv/dt の符号。ここで、(2) は 1 時間ごとに判定を行い、一致する時間の割合を求めた。この結果、(1) については、42.5% の CR で相関係数が 0.5 以上となり、(2) については、いずれも 'YES' が 'NO' を上回るとなった。この結果から、モデルと観測の不一致が現れるタイミングと内側境界条件設定過程との関係を考察し、SUSANOO-SW の境界条件設定モデル改良案についても議論する。

キーワード: 太陽風, 宇宙天気, MHD

Keywords: solar wind, space weather, MHD

非円形フラックスロープの不安定性に関する数値解析研究 Numerical Analysis of Instability of M-shape Flux Rope in the Solar Corona

石黒 直行^{1*}; 草野 完也¹
ISHIGURO, Naoyuki^{1*}; KUSANO, Kanya¹

¹ 名古屋大学 太陽地球環境研究所

¹Solar-Terrestrial Environment Laboratory, Nagoya University

The stability of magnetic flux rope in the solar corona is an important issue to understand the onset mechanism of solar flares and the formation of coronal mass ejections (CMEs). The instability of axisymmetric flux rope, called torus instability, is proposed to be the primary driver of solar eruption by Kliem and Toeroek (2006). They analyzed the ideal magnetohydrodynamic (MHD) stability of toroidal electric current channel for the mode of self-similar expansion, and concluded that the decay index of environmental magnetic field determines the criterion of the instability. However, several observations suggested that flux rope forms a non-axisymmetric loop in pre-eruptive state. In particular, the flux rope of M-shape structure, in which magnetic field line is concave above a magnetic polarity inversion line, is thought to be related to the onset of solar eruption. For instance, Moore et al. (2001) explained how the M-shape flux rope can be formed and erupts by tether-cutting reconnection. Recently, Kusano et al. (2012) found that the pre-flare reconnection between the sheared arcade and the small-scale magnetic flux of typical orientations favors the formation of M-shape flux rope and well triggers the tether-cutting reconnection scenario. However, the critical condition for the instability of the M-shape flux rope is still unclear.

In this paper, we numerically study the stability and dynamics of the M-shape flux rope. We model the M-shape flux rope using two current carrying tori which connect each other above the polarity inversion line and are anchored on the solar surface. The equilibrium condition is derived from the force balance of the hoop force of tori and the Lorentz force acting from external magnetic field. We also solve the equation of motion for the altitude of magnetic dip under the constraint that magnetic flux across the flux rope is conserved. As a result, the M-shape flux rope can be destabilized if the intensity of electric current exceeds the criterion and the altitude of magnetic dip ascends to the critical height. The numerical solution indicates that the decay index at the critical height of magnetic dip is substantially lower than the criterion of axisymmetric torus instability. It suggests that the M-shape flux rope much easily erupts than the theoretical prediction of axisymmetric torus instability, and the filament eruption may start even from a lower position where the decay index is lower than the conventional criterion.

Keywords: Sun, instability, flare, CME

プロミネンスからコロナキャビティに渡って成り立つ温度-密度間の冪乗則
Power-law relation between temperature and density in a prominence and a coronal cavity

金子 岳史^{1*}; 横山 央明¹
KANEKO, Takafumi^{1*}; YOKOYAMA, Takaaki¹

¹ 東京大学
¹The University of Tokyo

In this study, we discuss the formation mechanism of a solar prominence by the radiative condensation by using MHD simulations including optically thin radiative cooling and thermal conduction. Our main focus is on the relationship between the temperature and density in a prominence and its coronal cavity.

Solar prominences are the cool dense plasma clouds in the hot tenuous corona. The formation model of prominences has not been established completely. The radiative condensation is believed to be a key process.

In the previous study, we proposed a model through the radiative condensation triggered by the formation of a flux rope: The flux rope is formed by the reconnection after imposing converging and shearing motion on the footpoints of the coronal arcade field. The radiative condensation is triggered by the thermal nonequilibrium inside the flux rope. We have demonstrated this model in our simulations and found an empirical scaling law between the temperature and the density of a prominence.

The remained issues in our previous study were that the prominence in our simulations had much higher temperature than that of the observed one, and that the physical meaning of the scaling law was unclear due to the unrealistic small contrast of temperature and density between the prominence and the corona.

In this study, we allow the prominence temperature in our simulations to be lower, and reproduce more realistic prominences. As a result, we successfully extend the previous empirical scaling law to a power law both in a prominence and its surrounding coronal cavity. We also found that the power depends on the temperature gradient of each field line.

キーワード: 太陽プロミネンス, 太陽フィラメント
Keywords: solar prominence, solar filament

活動領域におけるコロナループ足下の遷移層で観測されるサブ秒角構造の特徴 Properties of sub-arcsecond transition-region structures at the footpoints of coronal loops in the active-region plane

木村 泰久^{1*}; 原 弘久²
KIMURA, Yasuhisa^{1*}; HARA, Hirohisa²

¹ 東京大学大学院, ² 国立天文台
¹University of Tokyo, ²National Astronomical Observatory of Japan

温度 5,800K の太陽光球上で起こるエネルギー解放が、外層の温度 $\sim 10,000$ K をもつ彩層と ~ 1 MK をもつコロナを形成する原因と考えられている。コロナの構造であるコロナループの足下は光球上の反極性を持つ磁場につながっており、多くの X 線、極紫外線望遠鏡で観測されているように、1 秒角以上の幅を持つことが分かっている。ひので衛星の極紫外線分光装置、EIS で観測されたコロナループ足下のフィリングファクターとドップラー速度から、ループ内部にはさらに小さい幅のループが存在することを示唆している。空間解像度 0.2 秒角を持つロケット観測望遠鏡 HiC の極紫外線撮像観測が、幅 1 秒角以上のコロナループの内部に示唆されているような微細構造があることを証明した。コロナ加熱を理解するためには、サブ秒角のコロナの構造を観測することが重要であるが、5 分間の HiC による観測以外に、要求される分解能のデータが無い。そこで我々は、サブ秒角の構造を詳しく調べるために Atmospheric Imaging Assembly (AIA) と Interface Region Imaging Spectrograph (IRIS) のデータを解析した。AIA のデータは空間分解能が 1.2 秒角、時間分解能が 12 秒である一方で、IRIS はコロナと彩層の間を空間分解能 0.3 秒角、時間分解能 10 秒で観測している。光球表面で kG の磁場を持つ活動領域プラージュの基底部分において、彩層からコロナまでに急激に温度が上がる非常に厚さの薄い領域である遷移層にコロナループの微細構造が繋がっていると考え、遷移層を撮像観測している IRIS の Si IV の輝線を用いた。結果として、間欠的に明るくなり、半値幅で 0.5-1.0 秒角程度の直径を持つ構造がコロナループ基底部分に普遍的に存在することが分かった。Si IV ラインの放射強度の変化が起こる位置は、コロナループ基底部分の断面の範囲内で時間とともに動くことが明らかとなった。さらに、AIA で観測したコロナループ基底部分の放射強度は、Si IV で観測されるサブ秒角の構造が出現した後、10-30 秒後に増光することが分かった。発表では、1 秒角より大きい幅を持つコロナループの内部でみられるサブ秒角の構造は何であるか、またその形成メカニズムについて考察したことを述べる。

キーワード: 太陽, コロナループ, 遷移層, IRIS
Keywords: sun, coronal loop, transition region, IRIS

初期太陽圏の物理状態について On Physical condition in the early Heliosphere

鈴木 建^{1*}
SUZUKI, Takeru^{1*}

¹ 名古屋大学 大学院理学研究科
¹ School of Science, Nagoya University

初期太陽圏の物理状態の進化について発表する。原始惑星系円盤の進化を、乱流駆動型円盤風の役割に焦点を当てつつレビューした後、太陽風の進化についての我々の結果を紹介する。さらに、太陽圏の物理状態の変化が、周囲の太陽系惑星の形成や進化に与える影響についても議論する。

キーワード: 太陽風, 原始惑星系円盤, 磁気流体力学, 波動, 乱流
Keywords: Solar Wind, Protoplanetary Disk, Magnetohydrodynamics, wave, turbulence

非一様場でのアルフベン波の衝撃波形成 Shock formation of Alfvén waves in a non-uniform medium

庄田 宗人^{1*}; 横山 央明¹
SHODA, Munehito^{1*}; YOKOYAMA, Takaaki¹

¹ 東京大学大学院理学系研究科地球惑星科学専攻
¹Department of Earth and Planetary Science, University of Tokyo

Alfvén waves, generated by photospheric granule motion, are considered to play a significant role in the energetics of coronal heating and solar wind acceleration. In many theoretical Alfvén wave models, coronal high temperature is supported by continuous energy supply by Alfvén waves and the ponderomotive force due to the local dissipation of Alfvén waves is responsible for solar wind acceleration. In linear theory dissipation due to viscosity and diffusivity is the only way to take out wave energy, which is too inefficient for coronal heating. Therefore some nonlinear processes such as phase mixing, shock formation and turbulent heating are the promising mechanisms for coronal heating and solar wind accelerations.

In this study we concentrate on shock heating among some nonlinear processes. The aim of our research is to estimate the shock formation time of Alfvén waves in a non-uniform medium. In case of uniform media, shock formation time is estimated analytically, while in non-uniform case it is not yet investigated sufficiently. We perform one-dimensional magnetohydrodynamic simulations for the estimation of shock formation time. A rightward-going Alfvénic wave packet of single wavelength is set initially and we calculate its nonlinear propagation. Background magnetic field is assumed to be uniform and only the density is set to be non-uniform in our simulation. The shock formation time is obtained by Fourier spectrum evolution. Due to the non-uniformity of the background, nonlinearity of Alfvén waves decreases as they propagate, which leads to the retardation and prevention of shock formation. We compare our numerical results with weakly nonlinear analytical results and show its validity. Analytical results, expressed by Lambert's W function, indicates that in the corona Alfvén waves hardly steepen, whereas in the interplanetary space the background condition is favorable for shock formation.

キーワード: アルフベン波, コロナ加熱, 太陽風
Keywords: Alfvén wave, coronal heating, solar wind

太陽彩層中における非線形アルフベン波の伝播および反射 Propagation and reflection of nonlinear Alfvén wave in the solar chromosphere

河野 隼也^{1*}; 横山 央明¹
KONO, Shunya^{1*}; YOKOYAMA, Takaaki¹

¹ 東京大学
¹The University of Tokyo

It has been suggested that Alfvén waves, generated in the photosphere and propagating along the magnetic flux tube, can carry enough energy to the low-plasma-beta region in the upper chromosphere and the dissipation of waves is one of the possible mechanisms to heat the solar chromosphere. Temperature of the chromosphere is low and the plasma gas is partially ionized. The collisions between plasmas and neutrals cause additional diffusion of the magnetic fields, which is called ambipolar diffusion. On the other hand, the compressible waves are generated by the nonlinear effect of the magnetic pressure associated with the Alfvén waves propagating upwards from the photosphere, and form shock waves in the chromosphere. In previous studies, it has been indicated that the dissipation of generated shock waves can give enough thermal energy to heat the chromosphere. The effect of the magnetic diffusion to the nonlinear propagation of Alfvén waves in the chromosphere has not been investigated enough. Some observations show the reflection of Alfvén waves at the top boundary of the chromosphere, which is called the transition region. It is important to discuss the dissipation mechanisms of waves in consideration of the reflection mechanism at the top and bottom boundaries of the chromosphere.

In this study, we investigate the reflection of Alfvén waves propagating along a vertically open magnetic flux tube in the chromosphere at the transition region and photosphere. If we assume the atmospheric condition in the solar quiet region, the damping length of waves which have frequencies of 1–100 mHz by the magnetic diffusion is estimated to become much larger than the thickness of the chromosphere. For investigating the dissipation of Alfvén waves in the chromosphere, we should consider the condition where the reflection at the photosphere and transition region efficiently occurs and more Alfvén waves are trapped in the chromosphere. We investigate the propagations of the nonlinear Alfvén waves by performing one-dimensional numerical simulations. As a result, 60–70 % of the incident Alfvénic pulse waves with frequencies of 10–100 mHz are reflected at the transition region. Most of reflected waves from the transition region penetrate into the convection zone without being reflected at the bottom of the photosphere. We perform simulations in different magnetic field structures and confirm that the results are almost the same in any cases. It is considered to be important to take the energy flux going from the top and bottom boundaries of the chromosphere into account for the dissipation of Alfvén waves in the chromosphere. In the case where the initial velocity amplitude of Alfvén wave is set to be 1.0 km s^{-1} , the compressible waves generated by the nonlinear effect may have enough energy to heat the chromosphere. If the initial velocity amplitude is set to be smaller, less compressible waves are generated and other dissipation mechanisms of the Alfvén waves may become effective.

キーワード: 彩層加熱, アルフベン波, 磁気拡散, 非線形
Keywords: chromospheric heating, Alfvén wave, magnetic diffusion, nonlinear

白色光増光現象を引き起こす太陽フレアの特徴 Characteristics that enhance white-light emission in solar flares

渡邊 恭子^{1*}; 増田 智²; 北川 潤²

WATANABE, Kyoko^{1*}; MASUDA, Satoshi²; KITAGAWA, Jun²

¹ 宇宙航空研究開発機構宇宙科学研究所, ² 名古屋大学太陽地球環境研究所

¹Institute of Space and Astronautical Science, Japan Aerospace Exploration Agency, ²Solar-Terrestrial Environment Laboratory, Nagoya University

In association with large (such as X-class) solar flares, we sometimes observe enhancements of visible continuum radiation, which is known as a "white-light flare". Because many white-light events show a close correlation between the time profiles and locations of white-light emission, and the hard X-rays and/or radio emission, it is believed that the origin of white-light emission is non-thermal electrons. However, not all large solar flares have white-light enhancements, and non-thermal electrons exist even in micro-flares. There should be some necessary condition to generate white-light enhancements.

To understand what conditions generate a white-light flare, we analyzed 42 M- and X-class flares observed with Hinode/SOT during the period from January 2011 to August 2013. Comparing the white-light (19 events) and no white-light (23 events) events, we concluded that the key factor needed to generate white-light enhancement is the precipitation of large amounts of nonthermal electrons into a compact region within a short time duration (Kitagawa et al., submitted to ApJ).

In this paper, we present the statistical results until December 2014. Not only the Hinode/SOT white-light (G-band (4305A) and continuum (Blue: 4505A, Green: 5550A, Red: 6684A)) data, but we also check SDO/HMI continuum data. The total number of events is now about twice that of Kitagawa's study. We compared the white-light emission data with GOES, hard X-ray emission data and/or the strength of the photospheric magnetic fields and looked for any relationship between them.

キーワード: 太陽フレア, 白色光, 粒子加速

Keywords: solar flare, white-light, particle acceleration

電波観測における白色光太陽フレアの特徴 Characteristics in solar white-light flares based on radio observations

増田 智^{1*}; 北川 潤¹; 渡邊 恭子²
MASUDA, Satoshi^{1*}; KITAGAWA, Jun¹; WATANABE, Kyoko²

¹ 名古屋大学太陽地球環境研究所, ² 宇宙航空研究開発機構宇宙科学研究所

¹Solar-Terrestrial Environment Laboratory, Nagoya University, ²Institute of Space and Astronautical Science, Japan Aerospace Exploration Agency

White-light flare is a solar flare in which an enhancement in white-light continuum is detected. Although most of white-light flares are large flares in energy like GOES X-class flare, it is not correct that only the amount of released energy determine if a solar flare becomes a white-light flare. To understand what generates a white-light flare, we analyzed 42 M- and X-class flares observed with Hinode/SOT during the period from January 2011 to August 2013. Among these 42 events, the number of white-light flares was 19. Comparing the white-light and no white-light events, we concluded that the key factor to generate white-light enhancement is the precipitation of large amount of nonthermal electrons within a short time duration into a compact region (Kitagawa et al., submitted to ApJ).

In this paper, we analyzed the 10 events (white-light: 4 events, no white-light: 6 events) among the 42 events, which were observed with Nobeyama Radio Heliograph (NoRH) and Nobeyama Radio Polarimeters (NoRP). GHz microwave are emitted by gyrosynchrotron from very-high energy (\sim MeV) accelerated electrons. The peak intensity in 17 and 35 GHz does not show any significant difference between the white-light and no white-light events. This indicates that such high-energy electrons does not contribute white-light enhancement. The spectrum of gyrosynchrotron emission usually has a peak frequency which corresponds to the turning point (turn-over frequency) between the optical thick part in the lower frequency range and the optically thin part in higher frequency range. The white-light flares show systematically high turn-over frequency than that of the no white-light events. The higher turn-over frequency might correspond to stronger magnetic field. This is consistent that white-light flares tend to be compact. As for the time evolution of the spectrum, the no white-light flares tend to show the spectral hardening. This indicates that the magnetic mirror effectively works in no white-light flares because of the weak magnetic field in the flare loop.

Keywords: solar flare, particle acceleration

太陽彩層における微小構造に関する二次元数値シミュレーション Two-dimensional simulation of the small scale structure in the solar chromosphere

飯島 陽久^{1*}; 横山 央明¹

IJIMA, Haruhisa^{1*}; YOKOYAMA, Takaaki¹

¹ 東京大学理学系研究科地球惑星科学専攻

¹Department of Earth and Planetary Science, Graduate School of Science, The University of Tokyo

Recent observation revealed the highly dynamic and fine structures in the solar chromosphere. The solar chromosphere is known to have wide range of the plasma beta, high nonlinearity with shock waves, cooling from the radiation, thermal conduction by the non-thermal electron, and weak ionization rate. All of the processes above have opportunity contributing to the dynamics of the solar chromosphere. In order to get the proper interpretation of the observation in the solar chromosphere, the numerical simulation with the various effects can be very useful tool. In our study, a new radiative magnetohydrodynamic code is developed for the dynamical simulation of the solar chromosphere. The numerical domain includes the upper part of the convection zone to the lower part of the corona. The convective motion as a driver of the dynamics in the upper atmosphere is consistently modeled using the radiative transfer calculation and the realistic equation of state. The thermal conduction from the non-thermal electron is also included. In this talk, we will report the numerical implementation from this numerical code and the first results filled with small scale structures in the two-dimensional domain.

Keywords: solar chromosphere, wave, convection, magnetohydrodynamics

野辺山45m電波望遠鏡によるミリ波の太陽彩層観測と宇宙天気 Millimetric observation of the solar chromosphere and space weather using the Nobeyama 45m radio telescope

岩井 一正^{1*}; 下条 圭美¹
IWAI, Kazumasa^{1*}; SHIMOJO, Masumi¹

¹ 国立天文台野辺山太陽電波観測所

¹ Nobeyama Solar Radio Observatory, National Astronomical Observatory

太陽彩層の大気構造は太陽大気の過熱機構や太陽面で発生する諸現象を理解するため基礎情報であり、宇宙天気の基礎研究として重要である。太陽からのミリ波の放射は、主に彩層からの熱制動放射である。この放射は局所熱力学平衡状態で形成され、Rayleigh-Jeansの法則が適用される波長である。また熱制動放射の光学的厚さは電子密度と温度で決まる。よってミリ波帯域を多波長で観測することで、輝度温度から放射領域の温度や密度といった大気構造を推定することが可能である。しかし、ミリ波・サブミリ波の大型望遠鏡の多くは太陽のような高い輝度の天体を観測することを想定して設計されていない。そのため、この波長帯での太陽の高空間分解観測は極めて稀である。本研究では、野辺山45m電波望遠鏡を用いて、85と115GHzにおいて黒点暗部を分解可能な空間分解可能な単面鏡観測を初めて行った。本研究では電波吸収体(ソーラーフィルター)を用いることで、受信機の飽和を回避した。観測の結果、ミリ波の輝度温度分布は活動領域・静穏領域の両方で紫外連続光(1700 Å)と極めて高い相関があることが分かった。黒点暗部の輝度温度の上限値は静穏領域と同程度であった。一方でプラージュ領域は静穏領域よりも高い輝度温度であった。45m電波望遠鏡のビームには、幅の広いサイドローブが存在する。加えて、黒点暗部はプラージュ領域に囲まれている。よって実際の黒点暗部の輝度温度は観測値より低いと考えられる。これはミリ波では黒点暗部は静穏領域よりも高い輝度温度であると予想する多くの彩層大気モデルと矛盾する。この結果は、実際の大気では、遷移層の高度が既存の大気モデルよりも低い可能性があることを示唆している。

キーワード: 太陽, 電波, ミリ波, 彩層, 宇宙天気

Keywords: Sun, Radio radiation, millimeter, Chromosphere, space weather

脈動オーロラ時に見られる広いエネルギー帯の電子散乱と中層大気への影響について
Wide energy electron precipitation associated with the pulsating aurora and its impact on the middle atmosphere

三好 由純^{1*}; 大山 伸一郎¹; 齊藤 慎司¹; 栗田 怜¹; 藤原 均²; 片岡 龍峰³; 海老原 祐輔⁴;
Kletzing Craig⁵; Reeves Geoff⁶; Santolik Ondrej⁷; Clilverd Mark⁸; Rodger Craig⁹; Turunen Esa¹⁰;
土屋 史紀¹¹
MIYOSHI, Yoshizumi^{1*}; OYAMA, Shin-ichiro¹; SAITO, Shinji¹; KURITA, Satoshi¹; FUJIWARA, Hitoshi²;
KATAOKA, Ryuho³; EBIHARA, Yusuke⁴; KLETZING, Craig⁵; REEVES, Geoff⁶; SANTOLIK, Ondrej⁷;
CLILVERD, Mark⁸; RODGER, Craig⁹; TURUNEN, Esa¹⁰; TSUCHIYA, Fuminori¹¹

¹名古屋大学太陽地球環境研究所, ²成蹊大学, ³国立極地研究所, ⁴京都大学生存圏研究所, ⁵アイオワ大学, ⁶ロスアラモス国立研究所, ⁷Charles University in Prague, Czech Rep., ⁸British Antarctic Survey, UK, ⁹University of Otago, NZ, ¹⁰Sodankyla Geophysical Observatory, University of Oulu, Finland, ¹¹東北大学大学院理学研究科惑星プラズマ・大気研究センター
¹Solar-Terrestrial Environment Laboratory, Nagoya University, ²Seikei University, ³National Institute of Polar Research, ⁴RISH, Kyoto University, ⁵University of Iowa, USA, ⁶Los Alamos National Laboratory, USA, ⁷Charles University in Prague, Czech Rep., ⁸British Antarctic Survey, UK, ⁹University of Otago, NZ, ¹⁰Sodankyla Geophysical Observatory, University of Oulu, Finland, ¹¹PPARC, Tohoku University

The pulsating aurora is caused by intermittent precipitations of tens keV electrons. It is also expected that not only tens keV electrons but also sub-relativistic/relativistic electrons precipitate simultaneously into the ionosphere owing to whistler-mode wave-particle interactions. We analyzed the pulsating aurora event in November 2012 using several ground-based observation data; EISCAT, riometer, and sub-ionospheric radio waves, and the Van Allen Probes satellite data. The electron density profile obtained from

the EISCAT Tromsø VHF radar identifies the electron density enhancement at >68 km altitudes. The electron energy spectrum derived from an inversion method indicates the wide energy electron precipitations from 10 keV - 200 keV. The riometer and network of sub-ionospheric radio wave observations also showed the energetic electron precipitations during this period. During this period, the footprint of the Van Allen Probe-A satellite was very close to Tromsø and the satellite observed rising tone emissions of the lower-band chorus (LBC) waves near the equatorial plane. Using the satellite observed LBC and trapped electrons as an initial condition, we conducted a computer simulation of the wave-particle interactions. The simulation showed simultaneous precipitation of electrons at both tens of keV and a few hundred keV, which is consistent with the energy spectrum estimated by the inversion method using the EISCAT observations. This result revealed that electrons with a wide energy range simultaneously precipitate into the ionosphere in association with the pulsating aurora. We also discuss the possible impacts on the middle atmosphere due to precipitations of wide energy electrons during the pulsating aurora.

キーワード: 電子降り込み, ジオスペース, 中層大気

Keywords: energetic electron precipitation, Geospace, middle atmosphere

太陽プロトンイベントでの航空機放射線被ばく Radiation dose of aircrews during solar proton events

片岡 龍峰^{1*}; 佐藤 達彦²
KATAOKA, Ryuho^{1*}; SATO, Tatsuhiko²

¹ 国立極地研究所, ² 日本原子力研究開発機構
¹National Institute of Polar Research, ²Japan Atomic Energy Agency

A significant enhancement of radiation doses is expected for aircrews during ground-level enhancement (GLE) events, while the possible radiation hazard remains an open question during non-GLE solar energetic particle (SEP) events. Using a new air-shower simulation driven by the proton flux data obtained from GOES satellites, we show the possibility of significant enhancement of the effective dose rate of up to 4.5 uSv/h at a conventional flight altitude of 12 km during the largest SEP event that did not cause a GLE. As a result, a new GOES-driven model is proposed to give an estimate of the contribution from the isotropic component of the radiation dose in the stratosphere during non-GLE SEP events. We show further development of our radiation dose model with some applications, including the most recent GLE 72 occurred on 16 Jan 2014.

キーワード: 太陽プロトンイベント, 放射線被ばく
Keywords: solar proton events, radiation dose

太陽高エネルギー粒子による中層大気中での微量化学種の変動：オゾンと硝酸 Variation of trace chemical species induced by solar energetic particles in the middle atmosphere: ozone and nitric acid

中井 陽一^{1*}; 望月 優子¹; 丸山 真美¹; 秋吉 英治²; 今村 隆史²

NAKAI, Yoichi^{1*}; MOTIZUKI, Yuko¹; MARUYAMA, Manami¹; AKIYOSHI, Hideharu²; IMAMURA, Takashi²

¹ 理研仁科加速器研究センター, ² 国立環境研究所

¹RIKEN Nishina Center, ²National Institute for Environmental Studies

Influences on the terrestrial environment of super solar flares have attracted interests recently. In a super solar flare, a large amount of protons, X-rays, gamma-rays etc. emitted from the surface of the sun intrude into the terrestrial atmosphere, which is called a solar energetic particle (SEP) event. In particular, high-energy protons come down to the stratosphere. The SEP protons can induce dissociation of nitrogen molecules. A part of dissociated nitrogen atoms contribute to increase of odd nitrogen oxides (NO_x) and reactive odd nitrogen species (NO_y). Consequently, the SEPs influence the ozone concentration through the chemical reactions in the atmosphere.

We have performed simulations for variation of chemical composition in SEP events by solving a large number of rate equations for concentrations of chemical species without taking into account of transport processes, i.e., simple Box-model simulations. More than 70 chemical species including ions and about 480 chemical reactions are adopted in the present simulation. A large number of ionic processes including recombination in the stratosphere were treated for the first time to our knowledge.

We assume that the energy deposits from the SEP protons to the chemical species determine the yields of prompt products. As a result, we can consider the prompt products to be generated from nitrogen and oxygen molecules of major components of the air. The estimation of the energy deposit is carried out using the calculations of ion-pair creation by the SEP protons [1]. For the yield estimation of the prompt products, the G-values are used [2,3], where the G-values are given by amount of products per absorbed energy of 100eV. During a SEP event, we deal with both the photochemical reactions and the reactions induced by the SEP protons in the simulation. Variation of chemical composition in a SEP event is estimated as a difference between the result of the simulation including the processes triggered by the SEP protons and that by taking account of only photochemical reactions.

In this talk, we will mainly report the results by our Box-model simulation for the variations of ozone and nitric acid for the SEP event observed in October-November 2003.

References

- [1] C.H. Jackman et al., *Atmos. Chem. Phys.* **8**, 765 (2008).
- [2] C. Willis and A. W. Boyd, *Int. J. Radiat. Phys. Chem.* **8**, 71 (1976).
- [3] H. Mätzing, *Adv. Chem. Phys.* **LXXX**, 315 (1991).

サイクル23/24における銀河宇宙線の太陽変調現象 The solar modulation of galactic cosmic rays during the cycle 23/24

三宅 晶子^{1*}; 柳田 昭平²

MIYAKE, Shoko^{1*}; YANAGITA, Shohei²

¹茨城工業高等専門学校, ²茨城大学理学部

¹National Institute of Technology, Ibaraki College, ²Ibaraki University, Faculty of Science

太陽圏内に進入したエネルギー数十 GeV 以下の銀河宇宙線は、太陽風や惑星間空間磁場による強度変動、すなわち太陽変調現象を生じる。宇宙線の強度は惑星間空間磁場の強度や極性、磁極の傾き、また太陽風速度の変化に合わせて変化するため、数値計算により銀河宇宙線太陽変調を再現・予測する場合にはこれらの変化を考慮に入れた計算が必要になる。

本発表では、サイクル23/24における銀河宇宙線の太陽変調現象の数値計算結果を報告し、極小期が予想される次期サイクルでの銀河宇宙線太陽変調の予測を議論する。

キーワード: 銀河宇宙線, 太陽変調, 太陽圏, 惑星間空間磁場

Keywords: galactic cosmic ray, solar modulation, heliosphere, Interplanetary magnetic field

マウンダー極小期の宇宙線強度変動 Variation of the intensity of galactic cosmic rays during the Maunder Minimum

宮原 ひろ子^{1*}; 堀内 一穂²; 門叶 冬樹³; 加藤 和浩³; 森谷 透³; 横山 祐典⁴; 松崎 浩之⁴;
本山 秀明⁵; 片岡 龍峰⁵
MIYAHARA, Hiroko^{1*}; HORIUCHI, Kazuho²; TOKANAI, Fuyuki³; KATO, Kazuhiro³; MORIYA, Toru³;
YOKOYAMA, Yusuke⁴; MATSUZAKI, Hiroyuki⁴; MOTOYAMA, Hideaki⁵; KATAOKA, Ryuho⁵

¹ 武蔵野美術大学, ² 弘前大学, ³ 山形大学, ⁴ 東京大学, ⁵ 国立極地研究所

¹Musashino Art Univ., ²Hirosaki Univ., ³Yamagata Univ., ⁴The Univ. of Tokyo, ⁵NIPR

Variations of the galactic cosmic-ray flux during the Maunder Minimum (AD1645-1715) are examined based on carbon-14 in tree rings and beryllium-10 in ice cores. Variations of beryllium-10 content in ice cores have suggested that the flux of galactic cosmic rays have increased by ~40 percent for about one year around every other solar cycle minima, when solar dipole magnetic field was negative. Periodicity of the events is ~26-28 years, corresponding to the Hale cycle during the Maunder Minimum. These extreme enhancements of cosmic rays are suggested to be possibly caused by a change in the large scale structure of heliospheric magnetic field, associated with extremely weakened solar activity. To obtain more reliable ages for those events, we have been also measuring the carbon-14 content in tree rings dated by dendro-chronology.

キーワード: マウンダー極小期, 宇宙線, 太陽活動, 太陽圏, 宇宙気候, 宇宙線生成核種

Keywords: Maunder Minimum, cosmic rays, solar activity, heliosphere, space climate, cosmogenic nuclide

Open Data of Sunspot and aurora records in the Chinese chronicles : 7th to 13th century Open Data of Sunspot and aurora records in the Chinese chronicles : 7th to 13th century

早川 尚志²; 玉澤 春史^{1*}; 河村 聡人¹; 磯部 洋明³

HAYAKAWA, Hisashi²; TAMAZAWA, Harufumi^{1*}; KAWAMURA, Akito D.¹; ISOBE, Hiroaki³

¹ 京都大学大学院理学研究科附属天文台, ² 京都大学大学院総合生存学館, ³ 京都大学宇宙総合学研ユニット

¹Kwasan and Hida Observatories, Graduate School of Science, Kyoto University, ²Graduate School of Advanced Integrated Studies in Human Survivability, Kyoto University, ³Kyoto University Unit of Synergetic Studies for Space

Records of sunspots and aurora observations in pre-telescopic historical documents can provide useful information about solar activity in the past. This is also true for extreme space weather events, as they may have been recorded as large sunspots observed by the naked eye or as low-latitude auroras. In this study, we present the results of a comprehensive survey of sunspots and aurora records in Chinese formal chronicles spanning the 7th to 13th . This chronicles contain records of continuous observations with well-formatted reports conducted as a policy of the government. A brief comparison of the frequency of sunspots and aurora observations and the observations of radioisotopes as an indicator of the solar activity during corresponding periods is provided. In our project, we survey and compile the sunspots and aurora records in historical documents from various locations and languages, ultimately providing it to the academic community, not only community of natural science but also human and social sciences, as open data.

Keywords: sunspot, aurora, archaeoastronomy, extrem space weather

巨大黒点 12192 はなぜコロナ質量放出を起こさなかったのか？ Why big sunspot 12192 did not produce CME ?

柴田 一成^{1*}; 石井 貴子¹; 河村 聡人¹
SHIBATA, Kazunari^{1*}; ISHII, Takako¹; KAWAMURA, Akito¹

¹ 京都大学理学研究科附属天文台

¹ Kwasan and Hida Observatories, Kyoto University

2014年10月下旬に出現した黒点12192の面積は $A = 2750 \text{ MSH} = \text{Millionth Solar}$

Hemisphereに達した。これは1990年11月の巨大黒点6368(面積 $A = 3080 \text{ MSH}$) 以来の

24年ぶりの巨大黒点であり、大フレアや大磁気嵐を起こす可能性があるとして、世界的な注目を集めた。実際、東のリムに見え始めた10月17日から西のリムに消えた10月30日までの2週間間に、Xクラスフレアを6回引き起こした。これは今サイクルにおいて、一活動領域当たりのXクラスフレアの数では最多であった。ところが、一見不思議なことに、これらの6回のXクラスフレアは、一つもコロナ質量放出(CME)を引き起こさず、その結果、太陽風はきわめて静かであり、磁気嵐は全く発生しなかった。

京大飛騨天文台では、この巨大黒点12192をSMART望遠鏡とドームレス太陽望遠鏡を用いて、詳細に観測し、6回のうちの2回のXクラスフレアの観測に成功した(10月19日UT5時3分(ピーク時) X1.1, 10月24日UT21時40分(ピーク時) X3.1)。

本講演では、飛騨天文台における上記の黒点とフレアの観測の概要を紹介するとともに、なぜこの巨大黒点のXクラスフレアはCMEを引き起こさなかったか、過去のCMEフレアと比較することにより統計的な観点から考察する。得られた結論を一言でまとめると、「同じX線強度のフレアに対しては、黒点が巨大になればなるほど、

CMEは発生しにくくなる」というものである。

キーワード: フレア, コロナ質量放出, 黒点, 磁場, 電磁流体力学, 宇宙天気予報

Keywords: flare, CME, sunspot, magnetic field, magnetohydrodynamics, space weather prediction

ひので衛星とSDO衛星から迫る太陽表面における磁場輸送 Investigation of surface magnetic flux transport by use of Hinode/SOT and SDO/HMI

飯田 佑輔^{1*}; 堀田 英之²

IIDA, Yusuke^{1*}; HOTTA, Hideyuki²

¹JAXA, ²HAO

¹Japan Aerospace Exploration Agency, ²High Altitude Observatory

Since magnetic field on the solar surface triggers various solar activities, it is very important to understand their structure in terms of the space weather. An important issue is transport mechanism of magnetic flux. It is thought that the flow dominates the magnetic field on the solar surface. Although the transport is treated as a pure diffusion process for long time, recent solar observations suggest the differences from the diffusion.

We reported the relationship between the travel distance of the magnetic flux concentration and the elapsed time from the birth of the concentrations. The sub-diffusion scaling was found in the time range longer than 2×10^4 seconds for the first time. The investigation is, however, limited because the analysis is done by using the magnetogram obtained by Solar Optical Telescope onboard the Hinode satellite (Hinode/SOT), which does NOT cover the whole Sun. Thus in this study we investigate the relationship with the Helioseismic and Magnetic Imager on board the Solar Dynamics Observatory (SDO/HMI), which covers the whole Sun. Since the spatial resolution of SDO/HMI is lower than that of Hinode/SOT, we use both telescopes in order to see the influence of the resolution on the analysis. We find the similar sub-diffusion scaling with the power law index of 0.7 ± 0.1 . SDO/HMI shows a slightly larger magnitude. This difference may come from the difference of spatial resolution between the telescopes. In the presentation, we also plan to show the 3D MHD simulation of the magneto-convection if time permits.

キーワード: 太陽, 対流, 磁場, 拡散

Keywords: Sun, convection, magnetic field, diffusion

太陽活動サイクルのフェーズと大きな宇宙天気イベントの発生について Solar cycle phase and occurrence of intense space weather events

巨 慎一^{1*}; 渡邊 堯¹

WATARI, Shinichi^{1*}; WATANABE, Takashi¹

¹ 情報通信研究機構

¹National Institute of Information and Communications Technology

黒点数であらわされる太陽活動サイクルの長さや形はサイクル毎に変化する。大きな宇宙天気イベントの太陽活動のフェーズに対する依存性を議論するためには、各太陽活動サイクルについて規格化をする必要がある。例えば、大きな宇宙天気イベントが、太陽活動サイクルで一様に起こるかどうか調べることは重要なことである。ここでは、太陽活動サイクルの長さ、立ち上がり時間、立下り時間を使って太陽活動サイクルの形の規格化を行った。大きな太陽フレアの発生、強い地磁気嵐の発生などについての解析結果について報告する。

キーワード: 太陽活動サイクル, 宇宙天気, 極端現象

Keywords: solar cycle, space weather, extreme event

宇宙天気事象時に電離圏地面電流回路で発達する電場・電流 Electric field and currents in the ionosphere-ground circuit during space weather disturbances

菊池 崇^{1*}; 橋本 久美子²; 海老原 祐輔³; 富澤 一郎⁴; 亘 慎一⁵

KIKUCHI, Takashi^{1*}; HASHIMOTO, Kumiko²; EBIHARA, Yusuke³; TOMIZAWA, Ichiro⁴; WATARI, Shinichi⁵

¹名古屋大学太陽地球環境研究所, ²吉備国際大学, ³京都大学生存圏研究所, ⁴電気通信大学宇宙電磁環境研究センター, ⁵情報通信研究機構

¹Nagoya University/Solar-Terrestrial Environment Laboratory, ²Kibi International University, ³Kyoto University, Research Institute for Sustainable Humanosphere, ⁴Center for Space Science and Radio Engineering, Univ. of Electro-Communications,

⁵National Institute of Information and Communications Technology

When the CME or CIR hit the magnetosphere, the electric field and currents are generated by the dynamos in the magnetosphere and transmitted to the polar ionosphere down the magnetic field lines and further to the low latitude ionosphere. The transmitted electric field drives the Hall currents that close with themselves in the high-midlatitude ionosphere and the field-aligned currents close with the Pedersen currents that extend to the equatorial ionosphere near-instantaneously, where the Pedersen currents are intensified considerably by the Cowling effect appearing as the equatorial electrojet (EEJ). Thus, the geomagnetic disturbances often appear concurrently at high latitudes and the dayside equator with magnitude decreasing with latitude but amplified at the equator. At midlatitudes, the electric fields transmitted from high latitude are detected with the HF Doppler sounder, which are well correlated with the EEJ. The concurrent development of the midlatitude electric field and EEJ is commonly observed during the storm sudden commencements (SC), geomagnetic PC and Pi pulsations, quasi-periodic DP2 and storm/substorm convection and overshielding events. As shown in this paper, disturbances in the GIC (geomagnetically induced currents) on the ground are also well correlated with the EEJ and electric field in the ionosphere. The observations suggest that the electric current flows from the dynamo in the magnetosphere into the ground via the ionosphere. The ionospheric currents and GIC are connected by the displacement currents flowing on the wave front of the TM₀ (TEM) mode waves propagating in the Earth-ionosphere waveguide (ionosphere-ground transmission line) [Kikuchi, 2014], where the Poynting flux is transported in the neutral atmosphere between the ionosphere and ground.

2014年12月の連発CMEに対する極冠域電離圏の応答: 2台の全天イメージャによる5日間連続モニタリング
Responses of polar cap ionosphere to successive CMEs in Dec 2014: 5 days continuous monitoring with two all-sky imagers

細川 敬祐^{1*}; 田口 聡²; 塩川 和夫³; 小川 泰信⁴; 大塚 雄一³
HOSOKAWA, Keisuke^{1*}; TAGUCHI, Satoshi²; SHIOKAWA, Kazuo³; OGAWA, Yasunobu⁴; OTSUKA, Yuichi³

¹電気通信大学, ²京都大学大学院理学研究科, ³名古屋大学太陽地球環境研究所, ⁴国立極地研究所
¹University of Electro-Communications, ²Graduate School of Science, Kyoto University, ³Solar-Terrestrial Environment Laboratory, Nagoya University, ⁴National Institute of Polar Research

In December 2014, three coronal mass ejections (CMEs) occurred successively during 4 days interval from December 18 to 21. These CMEs arrived at the Earth respectively at December 21, 22 and 23 and caused a small magnetic storm (Dst \sim -50 nT). During this interval, two all-sky airglow imagers were operative in Longyearbyen, Norway (78.1N, 15.5E) and Resolute Bay, Canada (74.7N, 265.1E) and monitoring the polar cap ionosphere continuously for 5 days from December 20 to 24. The two all-sky imagers observed continuous generation/propagation of polar cap patches from the dayside towards the nightside across the polar cap region during a prolonged interval of southward IMF Bz. Such a continuous transportation of high-density plasma is visualized for the first time. At the time of the arrival of second CME, the IMF Bz was directed strongly northward. During this period, the polar cap shrank significantly, which implies that the magnetosphere was almost closed during such a strongly northward IMF condition. By using the 5 days continuous optical data in the polar cap region, we will discuss various responses of polar cap ionosphere to CME-induced solar wind disturbances.

キーワード: 極冠域, 極冠パッチ, 極冠オーロラ, コロナ質量放出
Keywords: Polar cap, Polar cap patches, Polar cap aurora, Coronal Mass Ejection (CME)

宇宙線による新粒子生成促進についての重イオンビームでの検証実験 Laboratory experiment with heavy ion beam for verification of new particle formation by cosmic rays

鈴木 麻未^{1*}; 増田 公明¹; 伊藤 好孝¹; さこ 隆志¹; 松見 豊¹; 中山 智喜¹; 上田 紗也子¹;
三浦 和彦²; 草野 完也¹
SUZUKI, Asami^{1*}; MASUDA, Kimiaki¹; ITOW, Yoshitaka¹; SAKO, Takashi¹; MATSUMI, Yutaka¹;
NAKAYAMA, Tomoki¹; UEDA, Sayako¹; MIURA, Kazuhiko²; KUSANO, Kanya¹

¹ 名古屋大学太陽地球環境研究所, ² 東京理科大学

¹Solar-Terrestrial Environment Laboratory, Nagoya University, ²Tokyo university of science

It is considered that the solar activity may affect the global climate, but the correlation mechanism is still not understood. One of the possible mechanisms for the correlation is the cloud formation by the galactic cosmic rays, which are modulated by the variation of solar magnetic activity. This relation was clearly indicated by the good correlation observed for the galactic cosmic-ray intensity and the global low-cloud amount. This hypothesis includes the ion-induced nucleation model, in which new particles in the atmosphere are created efficiently through atmospheric ions produced by cosmic rays, and finally these particles grow up to the size of cloud condensation nuclei. In this study, a laboratory experiment for verification of the hypothesis has been conducted with a reaction chamber. A flow of clean air with water vapor, ozone and sulfuric dioxide was introduced to a metallic chamber, where we irradiated UV light for solar irradiance and beta rays or accelerator beam for cosmic rays. The beam of the heavy ion accelerator HIMAC at National Institute of Radiological Sciences was used in the present experiment.

The result so far showed that ion density in the chamber increased due to the heavy ion irradiation and enhancement of the number of aerosol particles due to its was confirmed. In this presentation, I will report the results of the heavy ion irradiation experiments. Heavy ion beam of nitrogen and xenon was used because their ionization loss is different by a factor of 60. The ionization loss could be an index representing the ability to ionize the air molecules that is, parameters that contribute to atmospheric ion generation. Since it is considered that the aerosol particle generation would be increased according to the amount of ions, the experiment was carried out for these ions. The results showed that produced ion density was not different for both ions with different ionization power, and aerosol particle production efficiency was almost the same. The less ionization density for Xe ions might be due to large recombination of produced ions along the ion beam tracks.

星雲遭遇による白亜紀末の寒冷化と大量絶滅 Global cooling and mass extinction driven by a dark cloud encounter

二村 徳宏^{1*}; 戎崎 俊一²; 丸山 茂徳³

NIMURA, Tokuhiro^{1*}; EBISUZAKI, Toshikazu²; MARUYAMA, Shigenori³

¹ 岡山天文博物館, ² 理化学研究所, ³ 東京工業大学 地球生命研究所

¹Okayama Astronomical Museum, ²RIKEN, ³Earth-Life Science Institute, Tokyo Institute of Technology

We found a broad positive anomaly in iridium across over ~5 m in a pelagic deep sea sediment core sample, in addition to a spike in iridium at the K-Pg boundary related to the Chicxulub asteroid impact. Any mixtures of materials on the surface of the Earth cannot explain the broad iridium component. On the other hand, we found that an encounter of the solar system with a giant molecular cloud can explain the component, if the molecular cloud has a size of ~100 pc and the central density of ~2000 protons/cc.

Kataoka *et al.* (2013; 2014) pointed that the encounter with a dark cloud may drive an environmental catastrophe to lead a mass extinction. The solid particles from the dark cloud accreted onto the Earth and stayed for several months or years in the stratosphere: Since their sunshield effect is as large as -9.3 W m^{-2} , it can be a cause of a global climate cooling in the last 8 Myr of Cretaceous period, which is suggested by the variations of stable isotope ratios in oxygen (Barrera & Savin, 1999; Li & Keller, 1999; 1998; Barrera & Huber, 1990) and strontium (Barrera & Savin, 1999; Ingram, 1995; Sugarman *et al.*, 1995). The resultant extensions of the continental ice sheet cause a regression of the sea level, too. The global cooling seems to be associated with the decrease in the diversity of fossils, which eventually lead to the mass extinction at the K-Pg boundary.

The mass extinction at K-Pg boundary is widely thought to be caused by an impact of an asteroid (Alvarez *et al.*, 1980; Schulte *et al.*, 2010) at 65.5 Ma. However, a complete extinction of the total family by just one asteroid impact seems rather difficult because of the following two reasons. (1) A severe environment turn-over would finish few years after impact, the solid particles and sulphate launched by the asteroid impact is settled down for only few months (troposphere) to few years (stratosphere) and negative radiative forcing become negligible after a few years from the impact. (2) There were similar impacts without environmental catastrophe on the Earth, for example, Woodleigh, Chesapeake and Popigai craters. However, there are no evidences of association for mass extinction. It is difficult to explain why only Chicxulub impact leads mass extinction but the other three comparable impacts did not.

It is worth noting that the encounter with the dark cloud can perturb the orbit of asteroids and comets by its gravitational potential may cause asteroid impact or comet shower. The asteroid impact at K-Pg, therefore, may be one of the consequences of the dark cloud encounter.

We conclude that the cause of the climate cooling at the End-Cretaceous was driven by an encounter with a giant molecular cloud, with such an encounter and related perturbation in global climate a more plausible explanation for the mass extinction than a single impact event, Chicxulub.

キーワード: 星雲の冬, 星雲遭遇, 宇宙気候学, 白亜紀末, K-Pg 境界, 大量絶滅

Keywords: Nebula Winter, dark cloud encounter, Space Climate, End-Cretaceous, K-Pg boundary, mass extinction

時系列予測機 UFCORIN を利用した GOES X 線ライトカーブにおける太陽フレア予報研究 Prediction Study of Solar Flare Events in GOES X-ray Flux using Time-Series Prediction Engine UFCORIN

村主 崇行^{1*}; 柴山 拓也²; 羽田 裕子³; 磯部 洋明⁴; 根本 茂⁵; 駒崎 健二⁵; 柴田 一成³
MURANUSHI, Takayuki^{1*}; SHIBAYAMA, Takuya²; HADA MURANUSHI, Yuko³; ISOBE, Hiroaki⁴;
NEMOTO, Shigeru⁵; KOMAZAKI, Kenji⁵; SHIBATA, Kazunari³

¹ 理化学研究所計算科学研究機構, ² 名古屋大学太陽地球環境研究所, ³ 京都大学大学院附属天文台, ⁴ 宇宙総合学研究ユニット, ⁵ 株式会社ブロードバンドタワー

¹RIKEN Advanced Institute for Computational Science, ²Solar-Terrestrial Environment Laboratory, Nagoya University, ³Kwasan and Hida Observatories, Kyoto University, ⁴Unit of Synergetic Studies for Space, ⁵BroadBand Tower, Inc.

We have been developing UFCORIN, an automated space weather prediction system based on machine-learning technologies. Our aim is twofold: one is to provide real-time space weather forecast that thoroughly utilize the huge amount of solar observation data available today. The other is to discover the observational flare-triggering features, by analyzing the big data with the clear goal of predicting the solar flares.

UFCORIN stands for Universal Forecast Constructor by Optimized Regression of INputs. As the name suggests, UFCORIN is designed as a generic time-series predictor, which can be set to predict arbitrary time series from arbitrary numbers and kinds of input time series.

Using our system we predict maximum of GOES X-ray flux for 24-hour period in the future. As inputs to the predictor, we use wavelet powers of the full disk line-of-sight magnetogram obtained by the Helioseismic and Magnetic Imager (HMI) on board the Solar Dynamic Observatory (SDO). We also use the total magnetic flux data by SDO/HMI, and past data of GOES X-ray flux as inputs. The simulated prediction ran for 2 years (2011-2012) with 1-hour time resolution. To predict X, $\geq M$ and $\geq C$ class flares events, we first predict the real value of the GOES X-ray flux maximum, and then apply different thresholds for different events. These thresholds are part of the prediction parameter subject to optimization.

Following Bloomfield et al. [2012], we use true skill statistics (TSS) to compare the performance of various prediction strategies. Our best TSS values using HMI and GOES data are 0.692, 0.470 and 0.566, respectively, for predicting X, $\geq M$ and $\geq C$ class flares. These TSS values are comparable to previous studies such as those by Song et al. [2009], by Bloomfield et al. [2012], and by Bobra & Couvidat [2014]. We emphasize that we predict flares for the 2-years continuous period, and make no use of active region detection. In contrast, all of the previous studies are based on active region images and selected set of events.

At the annual meeting, we would also like to report the progress of our ongoing research, for example the search of flare features in SDO/AIA ultraviolet images. Also, our techniques can be applied to the prediction of space weather events other than solar flares, such as solar wind, solar energetic particles, and geomagnetic disturbances. We are also trying to quantify the social and economic impacts of the solar flares, in order to provide customized space weather forecast for various human activities.

キーワード: 太陽フレア, 宇宙天気, フレア予測, SDO, ビッグデータ, 機械学習

Keywords: Solar flares, Space weather, Flare prediction, SDO, Big data, Machine learning

ニューラルネットワークを用いた太陽風入力による東京上空 foF2 の擾乱予測 Prediction of foF2 variation above Tokyo using solar wind input to a neural network

内田 ヘルベルト陽仁^{1*}; 三宅 亙²; 中村 真帆³
UCHIDA, Herbert Akihito^{1*}; MIYAKE, Wataru²; NAKAMURA, Maho³

¹ 東海大学大学院工学研究科, ² 東海大学工学部, ³ 東京学芸大学
¹Graduate School of Engineering, Tokai University, ²Tokai University, ³Tokyo Gakugei University

Neural network has the ability to learn the empirical relation from input data. It is often used to produce empirical prediction models of several space environmental parameters. One operational model (Nakamura, 2008) used K-index input to predict foF2 variations and ionosphere storms above Tokyo. There are also several works for predicting geomagnetic indices such as Dst from the solar wind inputs (e.g., Watanabe et al., 2002). These studies lead us to expect that the prediction of foF2 at the disturbed situation can be more accurate when solar wind parameters are used to the inputs. Recently the availability of solar wind parameters from the Advanced Composition Explorer became longer enough to overlap one solar activity. In this study, solar wind proton velocity and IMF-By, IMF-Bz are used to the input to predict the foF2 disturbances above Tokyo. The K-index input model (Nakamura, 2008) was also recreated using the same data term as the SW input model. The SW input model tends to predict more often the negative disturbance cases, and it predicted daytime quick variations more accurate than the K-index input model. Statistical comparison of the predicting ability of those 2 models will be discussed, and the contribution of the solar wind input parameters to the foF2 will be tested using an artificial input.

Keywords: ionosphere, foF2, prediction, neural network, solar wind

Prediction of MeV electron flux throughout the outer radiation belt by multivariate autoregressive model
Prediction of MeV electron flux throughout the outer radiation belt by multivariate autoregressive model

坂口 歌織^{1*}; 長妻 努¹; Spence Harlan²; Reeves Geoffrey³
SAKAGUCHI, Kaori^{1*}; NAGATSUMA, Tsutomu¹; SPENCE, Harlan²; REEVES, Geoffrey³

¹ 情報通信研究機構, ²University of New Hampshire, ³Los Alamos National Laboratory

¹National Institute of Information and Communications Technology, ²University of New Hampshire, ³Los Alamos National Laboratory

The radiation belts are consisted of relativistic energy electrons in MeV range. The electron flux in the outer belt is highly variable depending on both solar wind and magnetospheric conditions. Enhanced fluxes sometimes cause deep dielectric charging on spacecraft and therefore satellite anomaly happens after the discharge. Prediction of such MeV electron variations is needed for safety operation of the satellite in the near Earth's orbit, but the physical processes of acceleration, loss, and transport of relativistic electrons are not fully understood so far. Japanese space weather information center at NICT has developed a multivariate autoregressive (AR) model for the prediction of electron flux at geostationary orbit (GEO). The model can estimates future flux variations by a few days lagging response of solar wind parameter changes [Sakaguchi et al., 2013]. Now, we have developed new models to predict electron flux variation throughout the outer radiation belt at L=3-6. Observation data of 2.3 MeV electrons in 2012-2014 by Van Allen Probes are used as predictor time series variate. The appropriate combinations of explanation variate are examined and selected respectively for each of L value ($\Delta L=0.2$) model among geomagnetic indices (AE, Kp, Dst) as well as solar wind parameters (speed, BZ, BS, Pdyn). The combinations of these variates systematically change according to L-value shift. In the presentation, we show the estimation method of multivariate AR coefficient matrixes and discuss about estimated combinations of explanation variate. Also we show past prediction results that were validated by observation data based on two skill scores of prediction efficiency and persistence.

キーワード: radiation belt, prediction, Van Allen Probes

Keywords: radiation belt, prediction, Van Allen Probes

ひまわり8号に搭載された宇宙環境モニター (SEDA) による初期観測 Initial Observations of Space Environment Data Acquisition Monitor (SEDA) on Board Himawari-8

長妻 努^{1*}; 坂口 歌織¹; 久保 勇樹¹
NAGATSUMA, Tsutomu^{1*}; SAKAGUCHI, Kaori¹; KUBO, Yuki¹

¹ 情報通信研究機構

¹National Institute of Information and Communications Technology

New Japanese meteorological satellite, Himawari-8, was successfully launched on October 7, 2014. Space environment data acquisition monitor (SEDA) is on board Himawari-8, as one of the housekeeping information for satellite operation. SEDA consists two sensors. One is proton sensor, which has 8 separate diode detectors. The energy range of the proton detectors are from 21.6 MeV to 81.4 MeV.

The other is electron sensor, which measures internal charging currents caused by energetic electrons. There are eight sensor plates arranged in a stack and each plate responds to a different energy range. As a result, energetic electrons whose energy range between 0.2 to 4.5 MeV can be measured by the electron sensors. The time resolution of each sensors is 10 sec. The field of view of SEDA is eastward. Thus, the specification of SEDA is suitable for monitoring the energetic electrons and protons above Japanese meridian of Geostationary orbit.

Himawari-8/SEDA has been operating since November 3, 2014. Based on the agreement between Japanese Meteorological Agency (JMA) and NICT, JMA is providing Himawari/SEDA data in near-real time since January 21, 2015. Currently we are checking the quality of Himawari-8/SEDA data. Results of initial observation by Himawari-8/SEDA will be introduced in our presentation.

キーワード: 宇宙天気予報, ジオスペース, 放射線帯, プロトン現象, 高エネルギー粒子, 静止軌道

Keywords: Space Weather Forecast, Geospace, Radiation Belts, Proton Event, High Energy Particles, Geostationary Orbit

地表気温および気候テレコネクションパターンに対する太陽風の影響 Influence of solar wind on surface temperatures and climate teleconnection patterns

伊藤 公紀^{1*}

ITO, Kiminori^{1*}

¹ 横浜国立大学環境情報研究院

¹Yokohama National University

太陽風の気候影響を探るため、相関係数を地図化した相関地図を用い、太陽風強度の指標である地磁気擾乱指数 (aa 指数) と、地表気温および気候テレコネクションパターンとの関係を求めた。QBO (赤道域成層圏準二年振動) による層化を行い、可能な場合は太陽黒点数も考慮した。対象とした期間は、QBO 位相 (西風、東風) データの信頼性が高い 1942 年から 2014 年とした。相関の時間窓は最短 10 年、最長 73 年である。

図 1 に、1 月の aa 指数と 2 月の地表気温との相関地図の例を示す。時間窓は 1942 年～2014 年で、QBO の位相と黒点数 (大、中、小) で層化した。各条件により、異なる相関地図が得られている。北極振動や太平洋十年規模振動などのテレコネクションパターンと地表気温の相関地図と類似している場合も見られる。

このような検討の結果、太陽風の気候影響はテレコネクションパターンの気候影響と同程度であることが分かった。太陽風と北極振動の関係は良く知られているが、他のテレコネクションパターンとの相関も強い。直接あるいは間接に、太陽風が各テレコネクションパターンを励起していると考えられる。

キーワード: 太陽風, aa 指数, テレコネクションパターン, 地表気温, QBO

Keywords: solar wind, aa index, teleconnection pattern, surface temperature, QBO

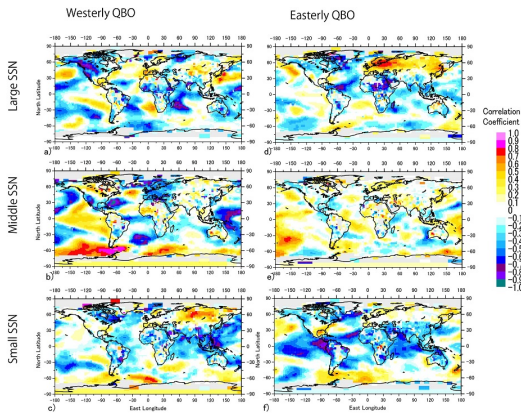


図 1. 相関地図の例。1 月 aa 指数と 2 月地表気温、期間は 1942～2014 年、QBO 位相 (西風、東風) と太陽黒点数 (大、中、小) で層化。